Desalination and Water Treatment
www.deswater.com
doi: 10.1080/19443994.2013.855678

53 (2015) 1395–1403
February

Taylor & Francis
Taylor & Francis Group

Characterization and sorption behavior of natural adsorbent for exclusion of chromium ions from industrial effluents

Mohammad Shahadat, Mohd. Rafatullah, Tjoon Tow Teng*

Division of Environmental Technology, School of Industrial Technology, Universiti Sains Malaysia, Penang 11800, Malaysia
Tel. +6046532215; Fax: +6046573678; email: ttteng@usm.my

Received 14 August 2013; Accepted 17 September 2013

ABSTRACT

A profuse agricultural biomass waste oil palm frond powder (OPFP) has been used as a stable extractor for the removal of chromium ions and characterized by using Fourier Transform Infrared (FTIR), Thermogravimetric analysis (TGA), X-ray diffraction (XRD), and Scanning electron microscopy (SEM) analyses. Batch adsorption experiments were employed to study the main parameters under various conditions (e.g. contact time, solution pH, initial metal ion concentration, temperature, etc.). The most favorable pH for the optimum sorption of chromium ion was found to be 4. Langmuir and Freundlich isotherms were tested to describe the adsorption mechanism. The monolayer adsorption capacity of OPFP for Cr(III) was found to be 119.04, 75.18, and 90.09 mg g^{-1} at 30, 40, and 50°C, respectively. Thermodynamic parameters were also computed and their results exposed the spontaneous and endothermic nature of sorption. FTIR confirmed that the interactions between metal ions and OPFP were responsible for adsorption. TGA indicated that no weight loss of mass was observed up to 300°C. XRD and SEM image showed amorphous morphology of untreated and metal-treated adsorbent. It was also found that after adsorption, the morphology of metal-treated OPFP had been completely changed which proved the phenomenon of adsorption. The low-cost thermally stable OPFP adsorbent has been successfully used for the removal of chromium ions from aqueous solutions.

Keywords: Oil palm frond; Characterization; Adsorption; Isotherm; Thermodynamic

1. Introduction

Water pollution due to heavy toxic metal ions has become a great anxiety for living beings owing to the human health hazards associated to their lethal caused [1]. Unlike organic pollutants, heavy metals are not biodegradable and tend to accumulate in living beings. Directly or indirectly, they are dispersed in natural water, accumulate in plants and animals, and finally in human beings through the food chain or by consumption of polluted water causing serious health hazards [2,3]. Heavy metals are a particular concern in the management of industrial wastewaters which include zinc, copper, nickel, mercury, cadmium, lead and chromium. So, heavy metal contamination has turned out to be the most remarkable environmental exertion of this century [4–6].

Among the heavy metal ions, chromium is the seventh most plentiful element on earth [7]. In the last few decades, the amount of chromium ions in aquatic and terrestrial ecosystems has been increased as a consequence of diverse anthropogenic activities (e.g. leather tannery, metal finishing, electroplating, stain-

*Corresponding author.

less steel production, textile industries, etc.). In the major toxic metal series, chromium is considered as the new entry after lead, cadmium, and mercury. Although chromium can exist in 11 valence states ranging from −IV to +VI [8], but Cr(III) and Cr(VI) play chief role in the environment owing to their stability. Cr(VI) is found to be 100 times more harmful than Cr (III) [9], prolonged exposure to Cr(III) could also cause skin allergies and cancer in human beings [10]. In addition, under certain conditions, Cr(III) can be oxidized to the state of more carcinogenic and mutagenic chromium(VI) by some bacteria or manganese oxide present in the environment [11]. The toxicological effect of Cr(VI) is also observed in the cell as an oxidizing agent as well as in the formation of free radical during reduction of Cr(VI) to Cr(III) [12]. The toxicity of Cr(VI) is the central theme of the Hollywood blockbuster movie "Erin Brockovitch." In the case of Hinkley (San Bernardino Country, USA), hexavalent chromium was used by Pacific Gas and Electric Company (PG & E) in the cooling system to prevent pipes from corrosion. The overflow of chromium contaminated water on the PG & E property leached into the ground and infected local water supplies. PG & E was required to compensate the plaintiffs $333 million, to clean up the chromium contamination and to stop using hexavalent chromium in their operations. This is the highest compensation award in metal toxicity history. A similar case occurred in 2007 in the Asopos River (near Oinofyta) Greece. In June 2009 (in Midland, Texas, USA), the ground water was found to be infected with chromium. The Indian Supreme court (in 2005) fined Hema chemicals for unlawful chromium discarding. So, the United States Environmental Protection Agency has put down the highest contaminant level for Cr (IV) in domestic water supplies to be 0.05 mg L^{-1} while the total Cr containing (e.g. Cr (III), Cr (VI)) and other species of chromium synchronized to be discharged below 2.0 mg L^{-1} [13].

Consequently, various treatment methods such as chemical precipitation, ion exchange, oxidation/reduction, liquid membrane adsorption, and biosorption have been developed for the removal of chromium [14–23]. The precipitation, oxidation/reduction, and lime neutralization have traditionally been the most frequently used methods. These technologies are moderately satisfactory in terms of removal of chromium from water, but these except a few produce solid residues. This toxic compound contains sludge whose final disposal is commonly done by land filling which is relatively of high costs and still a possibility of ground water contamination remains. Nonetheless, many of these attempts are marginally cost effective or difficult to be employed in developing countries. As a result, a treatment strategy should be simple, vigoros, and suitable for local resources and constraints [24]. So, attention has been paid to develop natural adsorbent for the removal of chromium ions from aqueous solutions.

Malaysia is the second largest palm oil producer in the world, covering plantation areas about 5.038 million hectares [25]. Oil palm tree (*Elaeis guineensis*) has become one of the most essential and precious commercial crops in Malaysia. Annually, the amount of lignocellulosic biomass is increasing because of palm oil plantation. In every 12 months, about 59 million tons palm oil biomass wastes by dry weight (including palm kernel shells and empty fruit brunches) were obtained at the time of replantation [26]. The main objective of this paper is to characterize oil palm frond powder (OPFP) and access its potential application for the removal and recovery of chromium ions from aqueous solutions.

2. Materials and methods

2.1. Raw materials (adsorbent)

The oil palm fronds were collected from FELDA oil palm plantation, Tenggaroh, Johor, Malaysia. The fronds were washed with demineralized water (DMW) to remove unwanted dust, soil, and insects prior to air-drying under sunlight. Oil palm fronds were then chopped into small strips by a vertical band saw and the size was reduced by using a hammer and chisel and being dried in oven (at 65 ± 2°C) for 24 h. The dried fronds were further ground to powder, washed with DMW, and filtered to remove the unwanted particles. The powder was dried at 65 ± 2°C for 24 h and sieved to retain on mesh sieve (250–500 μm). The powder was kept in a plastic bag and was stored in a desiccator for further use.

2.2. Chemicals and reagents

All chemicals used were of analytical reagent grade and were obtained from Sigma-Aldrich and Fluka (Germany). The stock solution (1,000 mg L^{-1}) of chromium(III) ions was prepared by dissolving their nitrate salt ($CrN_3O_9{\cdot}9H_2O$) in DMW. The solution was diluted to the required concentrations for further uses.

2.3. Apparatus

Infrared (IR) spectra of samples were recorded on a FTIR Spectrometer from Perkin Elmer (1730, USA) using KBr disc method. Thermogravimetric analysis/

differential thermal analysis (TGA/DTA) analysis was carried out by DTG – 60 H; C305743 00134, (Schimadzu, Japan) analyzer at a rate of 10°C min^{-1} in nitrogen atmosphere. An X' Pert PRO analytical diffractometer (PW-3040/60 Netherlands, Holland with CuK∝ radiation λ = 1.5418 Å) was used for X-ray diffraction (XRD) measurement. Scanning electron microscopy (SEM; Carl-Ziess SMT, Oberkochen, Germany) analysis was carried out on OPFP to study its surface morphology before and after adsorption of Cr(III) ions. A digital pH meter Elico EL-10 (Elico Malaysia) was used for pH measurements. Flame atomic absorption spectrometry (FAAS) measurements were made with a Model GBC-932-Plus flame atomic absorption spectrometer (GBC Scientific, Australia). A temperature-controlled shaker (MSW-275, India) was used for shaking. Muffle furnace (Narang Scientific works-India) was used for heating samples at different temperatures.

2.4. Adsorption studies

Batch adsorption studies were carried out by shaking 0.5 g of OPFP with 50 mL of the aqueous solutions of chromium ions for many times using a temperature-controlled shaker. The solution–adsorbents mixtures were stirred at 150 rpm and at the end of pre-determined time interval, the reaction mixtures were filtered out and analyzed for metal ion concentrations using Flame Atomic Absorption Spectrometer, FAAS. The effect of pH of the initial solution on equilibrium uptake of chromium ions was analyzed over a pH range from 1.0 to 6.0. The pH was adjusted using 0.1 M NaOH and 0.1 M HCI solutions. The adsorption experiments were also conducted to determine the equilibrium time, the optimum pH, and initial concentration of chromium ions for maximum adsorption. The percentage of metal adsorption by the adsorbents was computed using the equation:

$$\%\,\text{adsorption} = \{(C_i - C_e)/C_i\} \times 100 \quad (1)$$

where C_i and C_e are the initial and equilibrium concentration of metal ion (mg L^{-1}) in the solution, respectively. Adsorption capacity was calculated by using the mass balance equation for the adsorbent:

$$q = (C_i - C_e)V/W \quad (2)$$

where q is the adsorption capacity (mg g^{-1}), V is the volume of metal ion solution (L), and W is the weight of the adsorbent (g).

3. Results and discussion

3.1. Characterization of OPFP

3.1.1. Fourier Transform Infrared (FTIR) studies

FTIR analysis was done to identify the functional groups present in untreated and chromium-loaded OPFP and to examine the chemical changes before and after treatment of chromium ions solutions. A comparative FTIR spectrum (Fig. 1) show a broad peak in the region (3,200–3,550 cm^{-1}) which verify the presence of –OH group [27], whereas the peak at 2,916 cm^{-1} is attributed to C–H stretching [28]. The peaks with a maximum at 1,249 and 1,375 cm^{-1} prove the presence of lignin in the adsorbent [29] because lignin consists of guaiacyl (G) and syringyl propane units (S) which have one and two methoxy groups. The peak at 1,735 cm^{-1} is attributed to carbonyl groups while the peaks at 1,506, 1,457, 1,428, 1,109, and 1,062 cm^{-1} are assigned for the C–H deformations of the aromatic skeleton of lignin [30]. The syringyl ring breathing with CO stretching appears at 1,319 and 1,249 cm^{-1}. The spectrum of chromium-loaded OPFP also signifies that after loaded with metal ions, the functional groups of OPFP are slightly affected in their position and intensity. Table 1 summarizes the stretching vibrations of every peak before and after treatment of chromium ions solutions.

3.1.2. TGA studies

The thermal stability of native and chromium-loaded OPFP was scrutinized by TGA–DTA (Fig. 2). The TGA curve for untreated adsorbent shows only 6% weight loss up to 100°C. This is due to the exclusion of water molecules [31] from the adsorbent. One of the important features is observed from the TGA curve of unloaded OPFP; no weight loss of mass is observed from 200 to 300°C which indicates the high thermally stable nature of adsorbent. The weight loss from 250 to 390°C is a result of the complete breakdown of the organic part of the adsorbent. From 390°C onward, continuous weight loss of mass is due to alteration of the adsorbent into oxides. In comparison, in the TGA curve of native OPFP with chromium-loaded OPFP, no weight loss of mass is observed up to 300°C. The thermally stable characteristic property of chromium-loaded OPFP suggests that it can be effortlessly used in the industry at an elevated temperature.

3.1.3. X-ray and SEM analyses

X-ray analysis of untreated and chromium-loaded OPFP samples were carried out to provide information regarding amorphous and crystalline nature of the

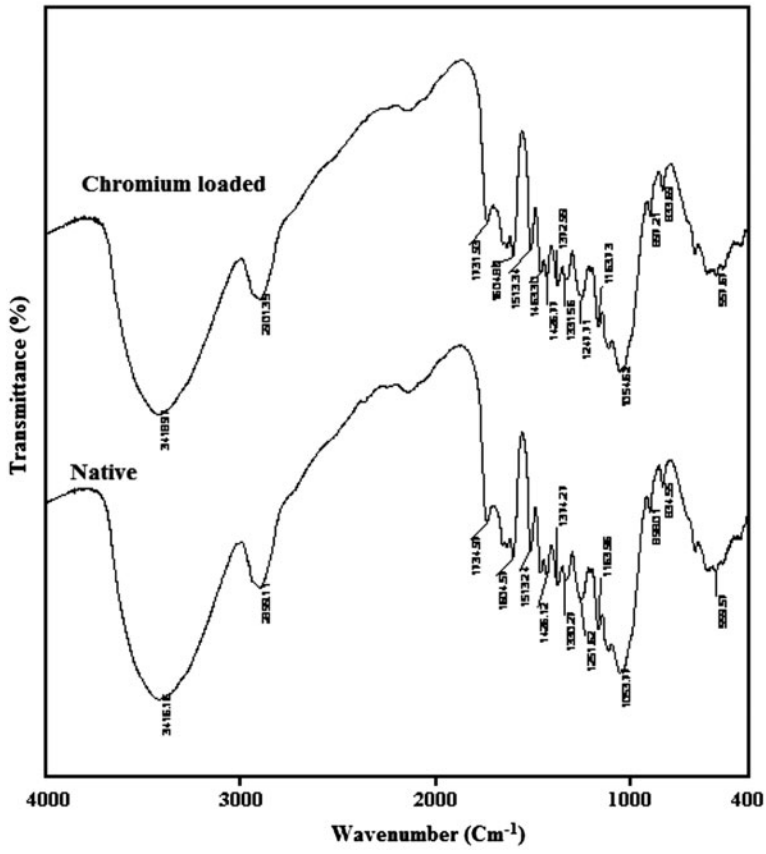

Fig. 1. A comparative FTIR spectra of chromium ions loaded and native OPFP adsorbent.

adsorbent. In the XRD patterns, no high or middle intensity peaks is observed (Fig. 3) which confirms the amorphous nature of both samples. The surface morphology of untreated and metal-treated samples was studied by SEM analysis. SEM images at different magnifications (Fig. 4) also confirm the amorphous morphology. SEM images show (Fig. 4(a and b)) that native OPFP exhibits a cave-like, irregular, and rough surface. However, after adsorption with chromium ion, the surface morphology of chromium-loaded OPFP (Fig. 4(c and d)) has been changed which is entirely different from the untreated OPFP, authenticating the adsorption of chromium ions on the surface of adsorbent.

3.2. Adsorption studies

3.2.1. Effect of contact time and initial chromium ions concentration

The effect of contact time and initial concentration of adsorbate on adsorption capacity was investigated to get the idea about the optimum absorption of chromium (III) ions on OPFP in shortest time. It is observed from Fig. 5 that the uptake of the metal ion increased simultaneously with the passage of contact time. Initially, the rate of absorption was fast. However, it gradually slowed down until reached equilibrium. This is due to the fact that a large number of vacant surface sites are available for adsorption during the initial stage. After a lapse of time, the remaining vacant surface sites are difficult to be occupied due to repulsive forces between the solute molecules of the solid and bulk phases. The maximum exclusion of chromium ions from aqueous solution was achieved after 120 min [32]. It is also evident from Fig. 5 that the amount of chromium ions adsorbed (mg g^{-1}) increased with increase in initial chromium ions concentration and remained constant after equilibrium time. The concentration difference provides an important driving force to overcome all mass transfer resistances of the chromium ions between the aqueous and solid phases. Hence, a higher initial concentration of chromium ions

Table 1
FTIR spectra of untreated and treated OPFP with Cr(III) ions

Frequency (before adsorption)	Frequency (after adsorption)	Possible functional group	Remarks
3411.22	3411.24	O–H (stretching)	Phenol group of cellulose, pectin, hemicellulose, lignin
2916.61	2918.40	C–H (stretching) 2˚ asymmetric carbon	Aliphatic compound. Methyl, methylene and methoxy groups
2135.32	2135.81	CΞC (stretching)	Alkynes
1735.54	1737.92	C=O (stretching)	Aldehyde, carboxylic acids or isolated carbonyl groups
1636.15	1635.75	C=C (symmetry) C=O (stretching)	Alkenes, aldehyde or quinines or carboxylic anhydrides
1506.76	1504.71	C=C (stretching)	Aromatic rings
1457.68	1455.63	C–H group in the plane deformation	Methyl, methylene or methoxy groups
1428.79	–		
1375.63	1382.99	CH_2 & CH_3 deformation	Alkanes
1319.96	1332.98		
1249.31	1249.59	C–O (stretching)	Alcohols, phenols and carboxylic acid
1162.63	1160.32		
1109.38	–		
1052.96	1049.94		
897.47	897.21	=CH (stretching)	Alkenes or benzene derivaties

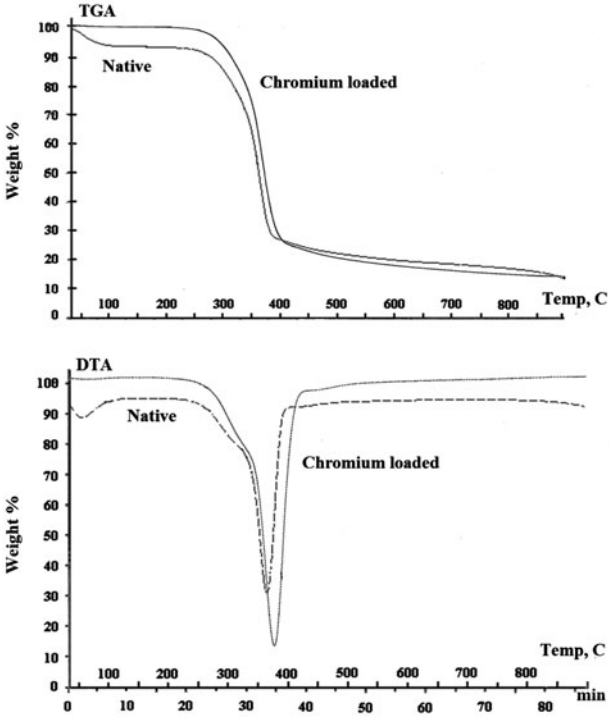

Fig. 2. TG-DTA curves of chromium ions loaded and native OPFP adsorbent.

enhances the adsorption process and the equilibrium adsorption capacity of OPFP increases with increase in initial metal ion concentration [33,34].

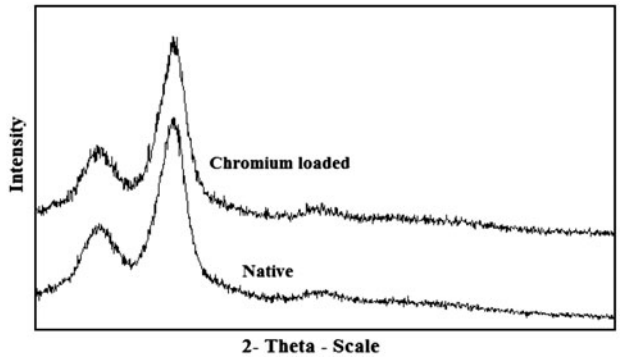

Fig. 3. XRD diffraction patterns of chromium ions loaded and native OPFP adsorbent.

3.2.2. *Effect of pH*

The pH of the solution is the most important parameter affecting metal ion adsorption. This is because of the competition of hydrogen ion with the positively charged metal ions on the active sites of the adsorbent. It is depicted in Fig. 6; initially, the adsorption capacity of chromium ions continuously increased and reached a maximum at pH 4.0, after that the percentage adsorption gradually decreased which may be due to the formation of metal hydroxides at higher pH.

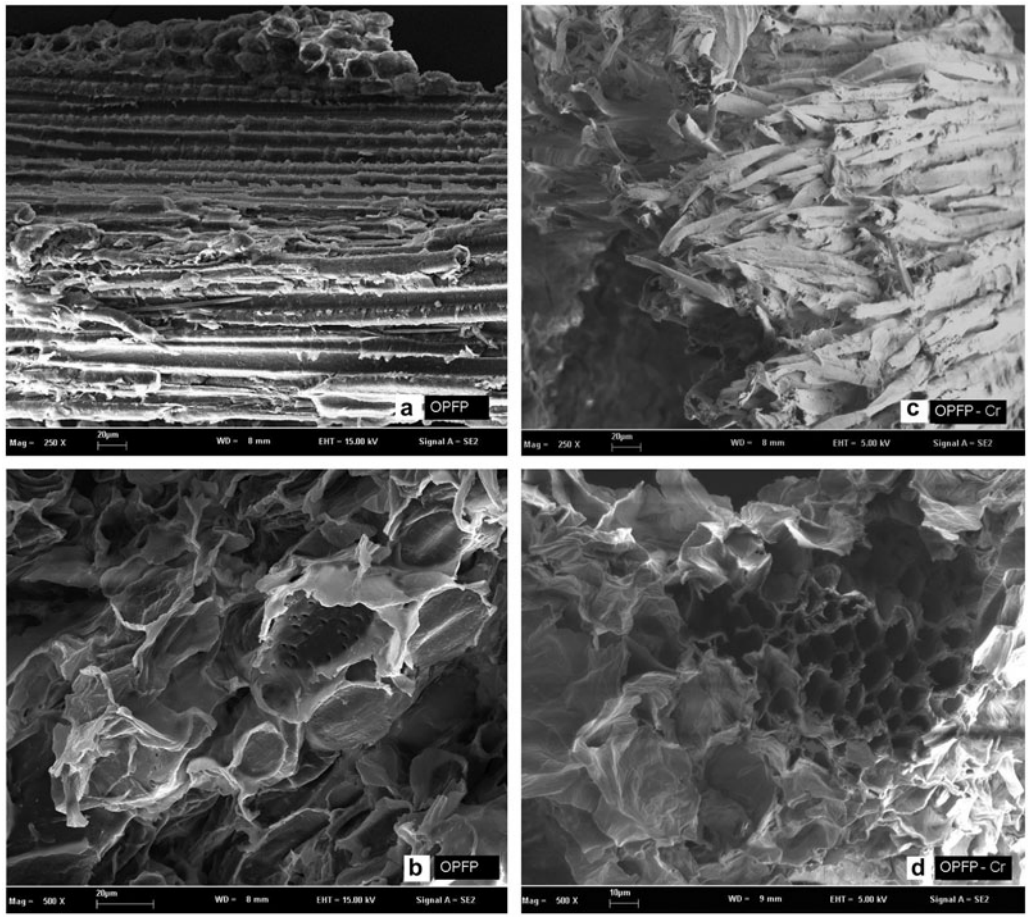

Fig. 4. SEM micrographs of native (a, b) and chromium ions loaded (c, d) OPFP adsorbent at different magnifications (250X and 500X).

3.3. Adsorption isotherm studies

To study the adsorption mechanism of OPFP for the removal of chromium (III) ions from aqueous solutions, the Langmuir and Freundlich adsorption isotherms models were used.

3.3.1. Langmuir adsorption model

This model assumes that the adsorptions occur at specific homogeneous sites on the adsorbent and is successfully used in monolayer molecular adsorption processes [35]. The data of the equilibrium adsorption of chromium ions onto OPFP may follow the following form of Langmuir model:

$$C_e/q_e = (1/b)(1/K_L) + (1/b)(C_e) \quad (3)$$

where C_e is the equilibrium concentration (mg L^{-1}) and q_e is the amount adsorbed per unit mass of adsorbent (mg g^{-1}), K_L is the Langmuir equilibrium constant that is related to the heat of adsorption and b is the monolayer capacity. Hence, a plot of C_e/q_e vs. C_e should be a straight line with a slope $(1/b)$ and an intercept as $(1/b.K_L)$ as shown in Fig. 7. The Langmuir-type adsorption isotherm indicates surface homogeneity of the adsorbent and hints toward the conclusion that the surface of the adsorbent is made up of small adsorption patches which are energetically equivalent to each other with respect to adsorption phenomenon. The correlation coefficient (R^2) values 0.987, 0.997, and 0.989, respectively, for 30, 40, and 50˚C indicate that the adsorption data of chromium (III) ions onto OPFP are well fitted to the Langmuir isotherm. The values of constants K_L and b are reported in Table 2.

3.3.2. Freundlich adsorption model

The Freundlich model can be applied for nonideal adsorption on heterogeneous surfaces and multilayer adsorption [36]. The Freundlich equations are:

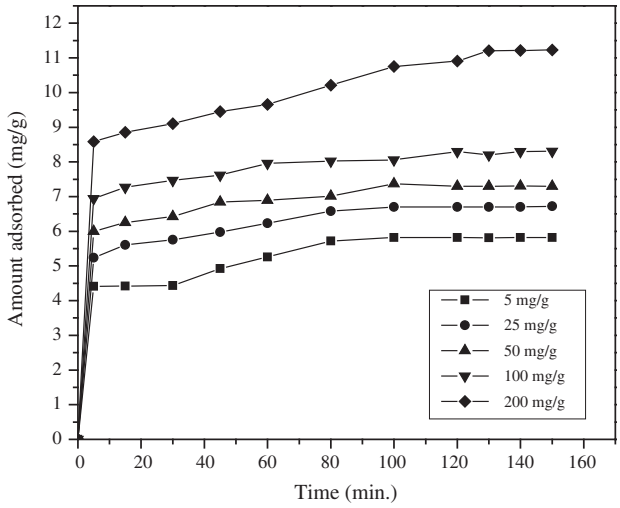

Fig. 5. Effect of contact time and initial concentration of chromium ions adsorption on OPFP.

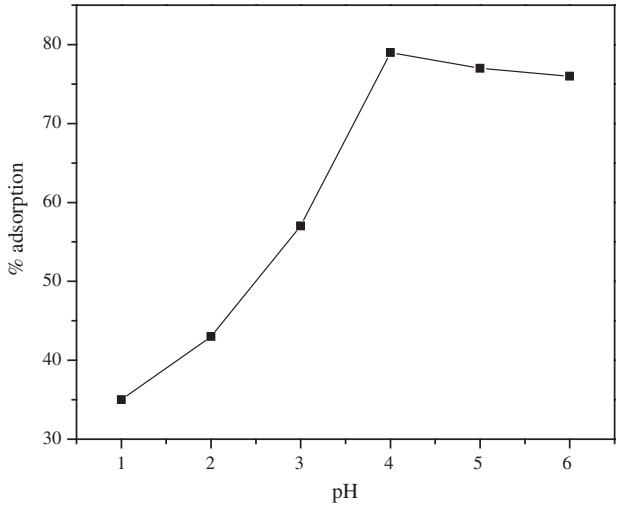

Fig. 6. Effect of the solution pH on chromium ions adsorption on OPFP.

$$q_e = (K_F)(C_e^{1/n}) \quad (4)$$

$$\ln q_e = \ln K_F + 1/n \ln C_e \quad (5)$$

where K_F is the measure of sorption capacity, $1/n$ is sorption intensity, and the rest of the terms have the usual significance. Thus, a plot of ln q_e vs. ln C_e should be a straight line with a slope $1/n$ and an intercept of ln K_F as shown in Fig. 8. The related parameters are reported in Table 2. The Freundlich-type adsorption isotherm is an indication of surface heterogeneity of the adsorbent and which is responsible for multilayer adsorption owing to the presence of energetically heterogeneous adsorption sites. From Table 2, the Langmuir adsorption isotherm model yields good fit as indicated by the R^2 values at all temperatures compared to the Freundlich adsorption isotherm models.

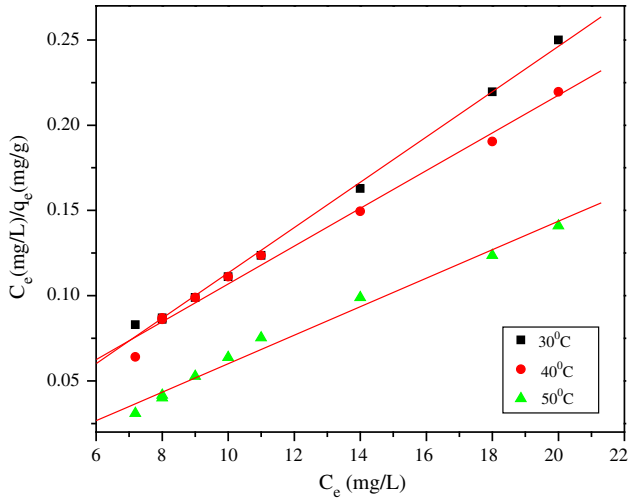

Fig. 7. Langmuir isotherm plots for the adsorption of chromium ions on OPFP at different temperatures.

Table 2
The related parameters for the adsorption of chromium (III) ions onto OPFP at different temperatures

Adsorption isotherms and its constants	Temperatures (°C)		
	30	40	50
Langmuir adsorption isotherm constants			
b (mg g^{-1})	119.04	75.18	90.09
K_L (L mg^{-1})	0.357	0.678	02.84
R^2	0.987	0.997	0.989
Freundlich adsorption isotherm constants			
K_F (mg g^{-1}) (L mg^{-1})$^{1/n}$	1.154	1.030	1.207
n	01.51	01.46	01.59
R^2	0.965	0.985	0.943

3.3.3 Thermodynamic studies

The standard free energy change is the fundamental criterion of spontaneity of a process. The Gibbs free energy (ΔG°), entropy (ΔS°), and enthalpy changes (ΔH°) of adsorption can be calculated by Van't Hoff and Gibbs-Helmholtz equations:

$$\Delta G^\circ = -\mathrm{RT} \ln K_L \quad (6)$$

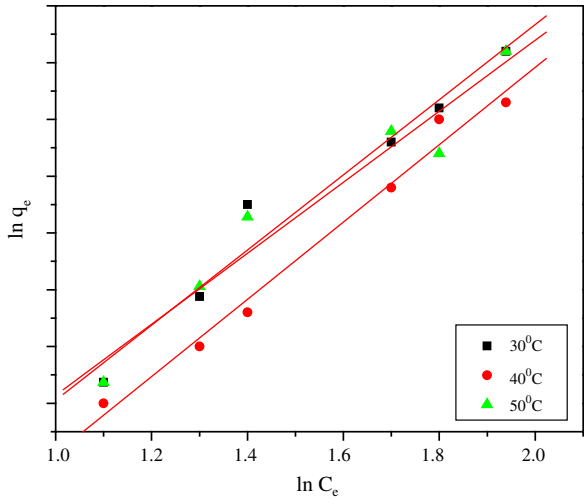

Fig. 8. Freundlich isotherm plots for the adsorption of chromium ions on OPFP at different temperatures.

where R is the universal gas constant (8.314 J mol^{-1} K^{-1}) and T is the absolute temperature (K) and K_L is the Langmuir equilibrium constant.

Similarly, the standard enthalpy change (from 303 to 323 K) was computed from the following equation:

$$\mathrm{Ln}\, K_L = \Delta S^\circ/R - \Delta H^\circ/\mathrm{RT} \quad (7)$$

A plot of ln K_L vs. $1/T$ should be a straight line as shown in Fig. 9 and the value of ΔH° and ΔS° can be calculated from the slope and intercept, respectively.

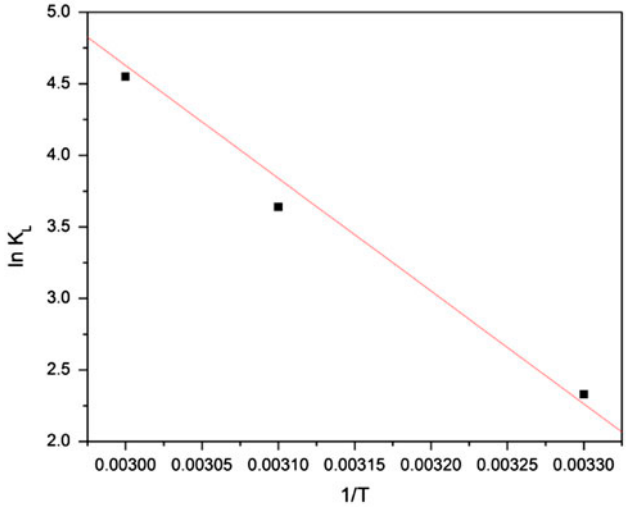

Fig. 9. Plot of ln K_L vs. $1/T$ for the adsorption of chromium ions on OPFP.

Table 3
The values of thermodynamic parameters for chromium (III) ions adsorption onto OPFP

Temp. (*K*)	ΔG° (kJ mol^{-1})	ΔH° (kJ mol^{-1})	ΔS° (kJ mol^{-1} K^{-1})	R^2
303	−7.358	60.51	0.218	0.992
313	−9.270			
323	−13.413			

The standard free energy change, standard enthalpy change, and standard entropy change are obtained from Eqs. (5) and (6) and their values associated with the adsorption of chromium ions onto OPFP are listed in Table 3. The negative values of ΔG° indicate the feasibility and spontaneous nature of the adsorption with a high performance of chromium ions on OPFP. The positive value of ΔH° and ΔS° indicates the endothermic and spontaneous nature, respectively. This behavior reflects the affinity of the adsorbents for the chromium ions and suggests some structural changes after adsorption. The value of n is found to be greater than unity which indicates favorable adsorption and supports the endothermic nature of adsorption of chromium ions onto OPFP.

4. Conclusions

Naturally occurring novel thermally stable adsorbent (OPFP) has been made by means of simple method and characterized by using sophisticated techniques. XRD and SEM analyses reveal amorphous morphology of treated and untreated OPFP whose structure has been completely changed after adsorption. The good thermally stable asset suggests that it can be used at the industry level at prominent temperature without loss of any mass. Equilibrium data fitted very well in the Langmuir isotherm equation, confirming the monolayer molecular adsorption of chromium ions onto OPFP with adsorption capacity of 119.04 mg g^{-1}. The thermodynamic calculations point toward the feasibility of the adsorption process with spontaneous and endothermic nature. On the basis of good findings, the naturally occurring OPFP can be used as an alternative for the removal of chromium ions from industrial waste as well as natural waste.

Acknowledgment

The authors would like to express their appreciations to Universiti Sains Malaysia for the financial support to this project via a short-term research grant (304/PTEKIND/6312008) and the Postdoctoral Fellowship to Mohammad Shahadat.

References

[1] F.V. Pereira, L.V.A. Gurgel, L.F. Gil, Removal of Zn^{2+} from aqueous single metal solutions and electroplating wastewater with wood sawdust and sugarcane bagasse modified with EDTA di-anhydride (EDTAD), J. Hazard. Mater. 176 (2010) 856–863.

[2] C.T. Chasapis, A.C. Loutsidou, C.A. Spiliopoulou, M.E. Stefanidou, Zinc and human health: An update, Arch. Toxicol. 86 (2012) 521–534.

[3] J. Watts, Lead poisoning cases spark riots in China, Lancet 374(9693) (2009) 868.

[4] N. Mañay, A.Z. Cousillas, C. Alvarez, T. Heller, Lead contamination in Uruguay: The La Teja neighborhood case. Reviews of environmental contamination and toxicology, Rev. Environ. Contam. T. 195 (2008) 93–115.

[5] F. Fenglian, Q. Wang, Removal of heavy metal ions from wastewaters: A review, J. Environ. Manage. 92 (2011) 407–418.

[6] L. Barbieri, A.C. Bonamartini, I. Lancellotti, Alkaline and alkaline—Earth silicate glasses and glass-ceramics from municipal and industrial wastes, J. Eur. Ceram. Soc. 20 (2000) 2477–2483.

[7] J.O. Nriagu, J.M. Pacyna, Quantitative assessment of worldwide contamination of air, water and soil by trace metals, Nature 333 (1998) 134–139.

[8] R. Fukai, Valency state of chromium in seawater, Nat.: London 213 (1967) 901.

[9] V. Gomez, M.P. Callao, Chromium determination and speciation since 2000, Trends Anal. Chem. 25 (2006) 1006–1015.

[10] Y.S. Yun, D. Park, J.M. Park, B. Volesky, Biosorption of trivalent chromium on the brown seaweed biomass, Environ. Sci. Technol. 35 (2001) 4353–4358.

[11] N. Sethunathan, M. Megharaj, L. Smith, S.P.B. Kamaludeen, S. Avudainayagam, R. Naidu, Microbial role in the failure of natural attenuation of chromium (VI) in long-term tannery waste contaminated soil, Agric. Ecosyst. Environ. 105 (2005) 657–661.

[12] A.K. Das, Micellar effect on the kinetics and mechanism of chromium(VI) oxidation of organic substrates, Coord. Chem. Rev. 248 (2004) 81–99.

[13] A. Baral, R.D. Engelken, Chromium-based regulations and greening in metal finishing industries in the USA, Environ. Sci. Policy 5 (2002) 121–133.

[14] Y.S. Woo, M. Rafatullah, A.F.M. Al-Karkhi, T.T. Tow, Removal of terasil red R dye by using Fenton oxidation: A statistical analysis, Desalin. Water Treat. (2010) 1–9.

[15] L.W. Man, P. Kumar, T.T. Teng, K.L. Wasewar, Design of experiments for malachite green dye removal from wastewater using thermolysis-coagulation-flocculation, Desalin. Water Treat. 40 (2012) 260–271.

[16] I. Ali, V.K. Gupta, Advances in water treatment by adsorption technology, Nat. London 1 (2006) 2661–2667.

[17] I. Ali, The quest for active carbon adsorbent substitutes: Inexpensive Adsorbents for toxic metal ions removal from wastewater, Sep. Purif. Rev. 39 (2010) 95–171.

[18] I. Ali, New generation adsorbents for water treatment, Chem. Rev. 112 (2012) 5073–5091.

[19] I. Ali, M. Asim, T.A. Khan, Low cost adsorbents for removal of organic pollutants from wastewater, J. Environ. Manage. 113 (2012) 170–183.

[20] I. Ali, Water treatment by adsorption columns: Evaluation at ground level, Sep. Purif. Rev. 43 (2014) 175–205.

[21] I. Ali, V. Kumar Gupta, I. Ali, A. Tawfik Saleh, M.N. Siddiqui, S. Agarwal, Chromium removal from water by activated carbon developed from waste rubber tires, Environ. Sci. Pollut. Res. 20 (2013) 1261–1268.

[22] V.K. Gupta, I. Ali, Removal of lead and chromium from wastewater using bagasse fly ash—A sugar industry waste, J. Colloid Interface Sci. 271 (2004) 321–328.

[23] M. Rafatullah, O. Sulaiman, R. Hashim, A. Ahmad, Adsorption of copper (II), chromium (II), nickel (II) and lead (II) ions from aqueous solutions by meranti sawdust, J. Hazard. Mater. 170 (2009) 969–977.

[24] D. Mohan, K.P. Singh, V.K. Singh, Trivalent chromium removal from wastewater using low cost activated carbon derived from agricultural waste material and activated carbon fabric cloth, J. Hazard. Mater. 135 (2006) 280–295.

[25] Economics & Industry Development Division Malaysian Palm Oil Board (MPOB) Report, June 2012.

[26] O. Sulaiman, N. Salim, N.A. Nordin, R. Hashim, M. Ibrahim, M. Sato, The potential of oil palm trunk biomass as an alternative source for compressed wood, Biol. Res. 7 (2012) 2688–2760.

[27] C.N.R. Rao, in: Chemical Application of Infrared spectroscopy, Academic Press, New York, NY, 1963, p. 355.

[28] L.L. Wang, G.T. Han, Y.M. Zhang, Comparative study of composition, structure and properties of *Apocynum venetum* fibers under different pretreatments, Carbohydr. Polym. 69 (2007) 391–397.

[29] J.X. Sun, X.F. Sun, R.C. Sun, F. Paul, S.B. Mark, Inhomogeneeities in the chemical structure of sugarcane bagasse lignin, J. Agric. Food Chem. 51 (2003) 6719–6725.

[30] R.M. Silverstein, G.C. Bassler, T.C. Morrill, Spectrometric identification of organic compounds, fourth ed., John Wiley and Sons, New York, NY, 1981 (Chapter 3), p.111.

[31] C. Duval, Inorganic Thermogravimetric Analysis, Elsevier, Amsterdam, 1963, p. 315.

[32] B.C. Meikap, K. Mohanty, J.T. Naidu, M.N. Biswas, Removal of crystal violet from wastewater by activated carbons prepared from rice husk, Ind. Eng. Chem. Res. 45 (2006) 5165–5171.

[33] B.H. Hameed, D.K. Mahmoud, A.L. Ahmad, Sorption of basic dye from aqueous solution by pamelo (Citrus grandis) peel in batch system, Colloids Surf. 316 (2008) 78–84.

[34] E.S.Z.E. Ashtoukhy, Loofa egyptiaca as a novel adsorbent for removal of direct blue dye from aqueous solution, J. Environ. Manage. 90 (2009) 2755–2761.

[35] I. Langmuir, The adsorption of gases on plane surfaces of glass, mica and platinum, J. Am. Chem. Soc. 40 (1981) 1361–1403.

[36] H. Freundlich, Over the adsorption in solutions, J. Phys. Chem. 57 (1907) 385–470.